Eur. Phys. J. C (2015) 75:30
DOI 10.1140/epjc/s10052-015-3265-4

THE EUROPEAN PHYSICAL JOURNAL C

Regular Article - Theoretical Physics

$D^*_{s1}(2860)$ and $D^*_{s3}(2860)$: candidates for $1D$ charmed-strange mesons

Qin-Tao Song[1,2,6], **Dian-Yong Chen**[1,2,a], **Xiang Liu**[2,3,b], **Takayuki Matsuki**[4,5,c]

[1] Nuclear Theory Group, Institute of Modern Physics, Chinese Academy of Sciences, Lanzhou 730000, China
[2] Research Center for Hadron and CSR Physics, Lanzhou University & Institute of Modern Physics of CAS, Lanzhou 730000, China
[3] School of Physical Science and Technology, Lanzhou University, Lanzhou 730000, China
[4] Tokyo Kasei University, 1-18-1 Kaga, Itabashi, Tokyo 173-8602, Japan
[5] Theoretical Research Division, Nishina Center, RIKEN, Saitama 351-0198, Japan
[6] University of Chinese Academy of Sciences, Beijing 100049, China

Received: 13 November 2014 / Accepted: 30 December 2014 / Published online: 27 January 2015

Abstract Newly observed two charmed-strange resonances, $D^*_{s1}(2860)$ and $D^*_{s3}(2860)$, are investigated by calculating their Okubo–Zweig–Iizuka-allowed strong decays, which shows that they are suitable candidates for the 1^3D_1 and 1^3D_3 states in the charmed-strange meson family. Our study also predicts other main decay modes of $D^*_{s1}(2860)$ and $D^*_{s3}(2860)$, which can be accessible at the future experiment. In addition, the decay behaviors of the spin partners of $D^*_{s1}(2860)$ and $D^*_{s3}(2860)$, i.e., $1D(2^-)$ and $1D'(2^-)$, are predicted in this work, which are still missing at present. The experimental search for the missing $1D(2^-)$ and $1D'(2^-)$ charmed-strange mesons is an intriguing and challenging task for further experiments.

1 Introduction

Very recently the LHCb Collaboration has released a new observation of an excess around 2.86 GeV in the $\bar{D}^0K^-$ invariant mass spectrum of $B^0_s \to \bar{D}^0K^-\pi^+$, which can be an admixture of spin-1 and spin-3 resonances corresponding to $D^*_{s1}(2860)$ and $D^*_{s3}(2860)$ [1,2], respectively. As indicated by LHCb [1,2], it is the first time to identify a spin-3 resonance. In addition, $D^*_{s2}(2573)$ also appears in the the $\bar{D}^0K^-$ invariant mass spectrum.

Before this observation, a charmed-strange state $D_{sJ}(2860)$ was reported by BaBar in the DK channel [3], where the mass and width are $m = 2856.6 \pm 1.5 \pm 5.0$ and $\Gamma = 47 \pm 7 \pm 10$ MeV [3], respectively, which was later confirmed by BaBar in the D^*K channel [4]. The $D_{sJ}(2860)$ has stimulated extensive discussions on its underlying structure. In Ref. [5], $D_{sJ}(2860)$ is suggested as a 1^3D_3 $c\bar{s}$ meson. This explanation was also supported by the study of the effective Lagrangian approach [6,7], the Regge phenomenology [8], the constituent quark model [9], and the mass loaded flux tube model [10]. The ratio $\Gamma(D_{sJ}(2860) \to D^*K)/\Gamma(D_{sJ}(2860) \to DK)$ was calculated as 0.36 [11] by the effective Lagrangian method. However, the calculation by the QPC model shows that such a ratio is about 0.8 [12], which is close to the experimental value $1.10 \pm 0.15 \pm 0.19$ [4]. Thus, a $J^P = 3^-$ assignment to $D_{sJ}(2860)$ is a possible explanation. In addition, $D_{sJ}(2860)$ as a mixture of charmed-strange states was given in Refs. [9,12,13]. $D_{sJ}(2860)$ could be a partner of $D_{s1}(2710)$, where both $D_{sJ}(2860)$ and $D_{s1}(2710)$ are a mixture of 2^3S_1 and 1^3D_1 $c\bar{s}$ states. By introducing such a mixing mechanism, the obtained ratio of D^*K/DK for $D_{sJ}(2860)$ and $D_{s1}(2710)$ [12] is consistent with the experimental data [4]. Reference [14] indicates that there exist two overlapping resonances (radially excited $J^P = 0^+$ and $J^P = 2^+$ $c\bar{s}$ states) at 2.86 GeV. Besides the above explanations under the conventional charmed-strange meson framework, $D_{sJ}(2860)$ was explained as a multiquark exotic state [15]. $D_{sJ}(2860)$ as a $J^P = 0^+$ charmed-strange meson was suggested in Ref. [5]. However, this scalar charmed-strange meson cannot decay into D^*K [5], which contradicts the BaBar's observation of $D_{sJ}(2860)$ in its D^*K decay channel [3]. After the observation of $D_{sJ}(2860)$, $D_{sJ}(3040)$ was reported by BaBar in the D^*K channel [4], which can be explained as the first radial excitation of $D_{s1}(2460)$ with $J^P = 1^+$ [16]. In addition, the decay behaviors of other missing $2P$ charmed-strange mesons in experiment were given in Ref. [16].

[a] e-mail: chendy@impcas.ac.cn
[b] e-mail: xiangliu@lzu.edu.cn
[c] e-mail: matsuki@tokyo-kasei.ac.jp

Briefly reviewing the research status of $D_{sJ}(2860)$, we notice that more theoretical and experimental efforts are still necessary to clarify the properties of $D_{sJ}(2860)$. It is obvious that the recent precise measurement of LHCb [1,2] provides us with a good opportunity to identify higher radial excitations in the charmed-strange meson family.

The resonance parameters of the newly observed $D^*_{s1}(2860)$ and $D^*_{s3}(2860)$ by LHCb include [1,2]:

$$m_{D^*_{s1}(2860)} = 2859 \pm 12 \pm 6 \pm 23 \text{ MeV}, \quad (1)$$

$$\Gamma_{D^*_{s1}(2860)} = 159 \pm 23 \pm 27 \pm 72 \text{ MeV}, \quad (2)$$

$$m_{D^*_{s3}(2860)} = 2860.5 \pm 2.6 \pm 2.5 \pm 6.0 \text{ MeV}, \quad (3)$$

$$\Gamma_{D^*_{s3}(2860)} = 53 \pm 7 \pm 4 \pm 6 \text{ MeV}, \quad (4)$$

where the errors are due to statistical one, experimentally systematic effects and model variations [1,2], respectively.

At present, there are good candidates for the $1S$ and $1P$ states in the charmed-strange meson family (see Particle Data Group for more details [17]). Thus, the two newly observed $D^*_{s1}(2860)$ and $D^*_{s3}(2860)$ can be categorized into the $1D$ charmed-strange states when considering their spin quantum numbers and masses. Before the observation of these two resonances, there were several theoretical predictions [18–21] of the mass spectrum of the $1D$ charmed-strange meson family, which are collected in Table 1. Comparing the experimental data of $D^*_{s1}(2860)$ and $D^*_{s3}(2860)$ with the theoretical results, we notice that the masses of $D^*_{s1}(2860)$ and $D^*_{s3}(2860)$ are comparable with the corresponding theoretical predictions, which further supports that it is reasonable to assign $D^*_{s1}(2860)$ and $D^*_{s3}(2860)$ as the $1D$ states of the charmed-strange meson family.

Although both the mass spectrum analysis and the measurement of the spin quantum number support $D^*_{s1}(2860)$ and $D^*_{s3}(2860)$ as the $1D$ states, we still need to carry out a further test of this assignment through study of their decay behaviors. This study can provide more detailed information on the partial decay widths, which is valuable for future experimental investigation of $D^*_{s1}(2860)$ and $D^*_{s3}(2860)$. In addition, there exist four $1D$ states in the charmed-strange meson family. At present, the spin partners of $D^*_{s1}(2860)$ and $D^*_{s3}(2860)$ are still missing in experiment. Thus, we will also predict the properties of the two missing $1D$ states in this work.

This paper is organized as follows. In Sect. 2, after some introduction we illustrate the study of decay behaviors of $D_{s1}(2860)$ and $D_{s3}(2860)$. In Sect. 3, the paper ends with the discussion and conclusions.

Table 1 Theoretical predictions for charmed-strange meson spectrum and comparison with the experimental data

$J^P(^{2s+1}L_J)$	Expt. [17]	GI [18]	MMS [19]	PE [20]	EFG [21]
$0^-(^1S_0)$	1968	1979	1967	1965	1969
$1^-(^3S_1)$	2112	2129	2110	2113	2111
$0^+(^3P_0)$	2318	2484	2325	2487	2509
$1^+(\text{“}^1P_1\text{”})$	2460	2459	2467	2535	2536
$1^+(\text{“}^3P_1\text{”})$	2536	2556	2525	2605	2574
$2^+(^3P_2)$	2573 [1,2]	2592	2568	2581	2571
$1^-(^3D_1)$	2859 [1,2]	2899	2817	2913	2913
$2^-(\text{“}^1D_2\text{”})$	–	2900	–	2900	2931
$2^-(\text{“}^3D_2\text{”})$	–	2926	2856	2953	2961
$3^-(^3D_3)$	2860 [1,2]	2917	–	2925	2871

2 Decay behavior of $D_{s1}(2860)$ and $D_{s3}(2860)$

Among all properties of these $1D$ states, their two-body Okubo–Zweig–Iizuka (OZI)-allowed strong decays are the most important and typical properties. Hence, in the following we mainly focus on the study of their OZI-allowed strong decays. For the $1D$ states studied in this work, their allowed decay channels are listed in Table 2. Among the four $1D$ states in the charmed-strange meson family, there are two $J^P = 2^-$ states, which is a mixture of 1^1D_2 and 1^3D_2 states, i.e.,

$$\begin{pmatrix} 1D(2^-) \\ 1D'(2^-) \end{pmatrix} = \begin{pmatrix} \cos\theta_{1D} & \sin\theta_{1D} \\ -\sin\theta_{1D} & \cos\theta_{1D} \end{pmatrix} \begin{pmatrix} 1^3D_2 \\ 1^1D_2 \end{pmatrix}, \quad (5)$$

where θ_{1D} is a mixing angle. In the heavy quark limit, a general mixing angle between ^3L_L and ^1L_L is $\theta_L = \arctan(\sqrt{L/(L+1)})$, which indicates $\theta_{1D} = 39^\circ$ [22].

In the following, we apply the quark pair creation (QPC) model [23–33] to describe the OZI-allowed two-body strong decays shown in Table 2, where the QPC model was extensively adopted to study the strong decay of hadrons [5,16,34–43]. In the QPC model, the quark–antiquark pair is created in QCD vacuum with vacuum quantum number $J^{PC} = 0^{++}$. For a decay process, i.e., an initial observed meson

Table 2 The two-body OZI-allowed decay modes of the $1D$ charmed-strange mesons. Here, we use symbols, ∘ and –, to mark the OZI-allowed and OZI-forbidden decay modes, respectively. $D^*_{s1}(2860)$ and $D^*_{s3}(2860)$ are 1^3D_1 and 1^3D_3 states, respectively

Channels	$D^*_{s1}(2860)$	$1D(2^-)$ $1D'(2^-)$	$D^*_{s3}(2860)$
DK	∘	–	∘
D^*K	∘	∘	∘
$D_s\eta$	∘	–	∘
$D^*_s\eta$	∘	∘	∘
DK^*	∘	∘	∘
$D^*_0(2400)K$	–	∘	–
$D^*_{s0}(2317)\eta$	–	∘	–

Table 3 The R values (in units of GeV^{-1}) [46] and masses (in units of MeV) [17] of the mesons involved in present calculation

States	R	Mass	States	R	Mass	States	R	Mass
D	2.33	1867	D^*	2.70	2008	$D_0(2400)$	3.13	2318
D_s	1.92	1968	D_s^*	2.22	2112	$D_{s0}(2317)$	2.70	2318
K	2.17	494	K^*	3.13	896	η	2.12	548

A decaying into two observed mesons B and C, the process can be expressed as

$$\langle BC|T|A\rangle = \delta^3(\mathbf{P}_B + \mathbf{P}_C)\mathcal{M}^{M_{J_A}M_{J_B}M_{J_C}}, \tag{6}$$

where $\mathbf{P}_B(\mathbf{P}_C)$ is the three-momentum of the final meson $B(C)$ in the rest frame of A. $M_{J_i}(i = A, B, C)$ denotes the orbital magnetic momentum. Additionally, $\mathcal{M}^{M_{J_A}M_{J_B}M_{J_C}}$ is the helicity amplitude. The transition operator T in Eq. (6) is written as [23–33]

$$T = -3\gamma \sum_m \langle 1m; 1-m|00\rangle \int \mathrm{d}\mathbf{p}_3 \mathrm{d}\mathbf{p}_4 \delta^3(\mathbf{p}_3 + \mathbf{p}_4) \times \mathcal{Y}_{1m}\left(\frac{\mathbf{p}_3 - \mathbf{p}_4}{2}\right) \chi^{34}_{1,-m}\phi^{34}_0\omega^{34}_0 b^\dagger_{3i}(\mathbf{p}_3)\mathrm{d}^\dagger_{4j}(\mathbf{p}_4), \tag{7}$$

which is introduced in a phenomenological way to reflect the property of quark-antiquark (denoted by indices 3 and 4) created from vacuum. $\mathcal{Y}_{lm}(\mathbf{p}) = |\mathbf{p}|Y_{lm}(\mathbf{p})$ is the solid harmonic. χ, ϕ, and ω are the general description of the spin, flavor, and color wave functions, respectively.

By the Jacob–Wick formula [44], the decay amplitude reads

$$\mathcal{M}^{JL}(\mathbf{P}) = \frac{\sqrt{2L+1}}{2J_A+1} \sum_{M_{J_B}M_{J_C}} \langle L0; JM_{J_A}|J_A M_{J_A}\rangle \times \langle J_B M_{J_B}; J_C M_{J_C}|J_A M_{J_A}\rangle \mathcal{M}^{M_{J_A}M_{J_B}M_{J_C}}. \tag{8}$$

Finally, the general decay width is

$$\Gamma = \pi^2 \frac{|\mathbf{P}_B|}{m_A^2} \sum_{J,L} |\mathcal{M}^{JL}(\mathbf{P})|^2, \tag{9}$$

where m_A is the mass of the initial state A. In the following, the helicity amplitudes $\mathcal{M}^{M_{J_A}M_{J_B}M_{J_C}}$ of the OZI-allowed strong decay channels in Table 2 are calculated, which is the main task of the whole calculation. Here, we adopt the simple harmonic oscillator (SHO) wave function $\Psi_{n,\ell m}(\mathbf{k})$, where the value of a parameter R appearing in the SHO wave function can be obtained such that it reproduces the realistic root mean square (rms) radius, which can be calculated by the relativistic quark model [46] with a Coulomb plus linear confining potential as well as a hyperfine interaction term. In Table 3, we list the R values adopted in our calculation. The strength of $q\bar{q}$ is taken as $\gamma = 6.3$ [16] while the strength of $s\bar{s}$ satisfies $\gamma_s = \gamma/\sqrt{3}$. We need to specify our γ value adopted in the present work which is $\sqrt{96\pi}$ times larger than that adopted by other groups [45,46], where the γ value as an overall factor can be obtained by fitting the experimental data (see Ref. [47] for more details of how to get the γ value).

In addition, the constituent quark masses for charm, up/down, and strange quarks are 1.60, 0.33, and 0.55 GeV, respectively [46].

With the above preparation, we obtain the total and partial decay widths of $D_{s1}^*(2860)$, $D_{s3}^*(2860)$, and their spin partners, and comparison with the experimental data [1,2]. As shown in Table 3, the R value of the P-wave charmed-strange meson is about $2.70\,\mathrm{GeV}^{-1}$. For the D-wave state, the R value is estimated to be around $3.00\,\mathrm{GeV}^{-1}$ [46]. In present calculation, we vary the R value for the D-wave charmed-strange meson from 2.4 to $3.6\,\mathrm{GeV}^{-1}$. In Fig. 1, we present the R dependence of the total and partial decay widths of $D_{s1}(2860)$ and $D_{s3}(2860)$.

2.1 $D_{s1}(2860)$

The total width of $D_{s1}(2860)$ as the 1^3D_1 state is given in Fig. 1, where the total width is obtained as $128 \sim 177$ MeV corresponding to the selected R range, which is consistent with the experimental width of $D_{s1}(2860)$ ($\Gamma = 159 \pm 23 \pm 27 \pm 72$ MeV [1,2]). The information of the partial decay widths depicted in Fig. 1 also shows that DK is the dominant decay mode of the 1^3D_1 charm strange meson, which explains why $D_{s1}(2860)$ was experimentally observed in its DK decay channel [1,2]). In addition, our study also indicates that the D^*K and DK^* channels are also important for the 1^3D_1 state, which have partial widths $35 \sim 44$ and $24 \sim 40$ MeV, respectively. The $D_s\eta$ and $D_s^*\eta$ channels have partial decay widths with several MeV, which is far smaller than the partial decay widths of the DK, D^*K, and DK^* channels. This phenomenon can be understood since the decays of the 1^3D_1 state into $D_s\eta$ and $D_s^*\eta$ have a smaller phase space.

The above results show that $D_{s1}(2860)$ can be a good candidate for the 1^3D_1 charmed-strange meson.

Besides providing the partial decay widths, we also predict several typical ratios, i.e.,

$$\frac{\Gamma(D_{s1}(2860) \to D^*K)}{\Gamma(D_{s1}(2860) \to DK)} = 0.46 \sim 0.70, \tag{10}$$

$$\frac{\Gamma(D_{s1}(2860) \to DK^*)}{\Gamma(D_{s1}(2860) \to DK)} = 0.25 \sim 0.85, \tag{11}$$

$$\frac{\Gamma(D_{s1}(2860) \to D_s\eta)}{\Gamma(D_{s1}(2860) \to DK)} = 0.10 \sim 0.14, \tag{12}$$

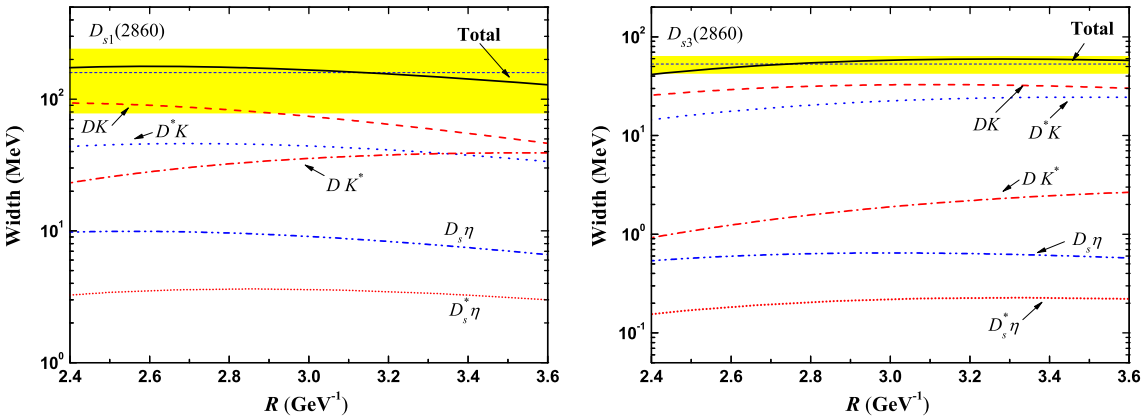

Fig. 1 The total and partial decay widths of 1^3D_1 (*left panel*) and 1^3D_3 (*right panel*) charmed-strange mesons dependent on the R value. Here, the *dashed lines* with the *yellow bands* are the experimental widths of $D_{s1}^*(2860)$ and $D_{s3}^*(2860)$ from LHCb [1,2]

which can be further tested in the coming experimental measurements.

The Belle Collaboration once reported $D_{s1}(2710)$ in the DK invariant mass spectrum, which has mass $2708 \pm 9^{+11}_{-10}$ MeV and width $108 \pm 23^{+36}_{-31}$ MeV [48]. The analysis of angular distribution indicates that $D_{s1}(2710)$ has the spin-parity $J^P = 1^-$ [48]. Later, the BaBar Collaboration confirmed $D_{s1}(2710)$ in a new D^*K channel [4], where the ratio $\Gamma(D^*K)/\Gamma(DK) = 0.91 \pm 0.13 \pm 0.12$ for $D_{s1}(2710)$.

In Refs. [5,11], the assignment of $D_{s1}(2710)$ to the 1^3D_1 charmed-strange meson was proposed. However, the obtained $\Gamma(D^*K)/\Gamma(DK) = 0.043$ [11] is deviated far from the experimental data, which does not support the 1^3D_1 charmed-strange assignment to $D_{s1}(2710)$. Especially, the present study of newly observed $D_{s1}(2860)$ shows that $D_{s1}(2860)$ is a good candidate of the 1^3D_1 charmed-strange meson.

If $D_{s1}(2710)$ is not a 1^3D_1 charmed-strange meson, we need to find the place in the charmed-strange meson family. In Ref. [5], the authors once indicated that $D_{s1}(2710)$ as the 2^3S_1 charmed-strange meson is not completely excluded.[1] By the effective Lagrangian approach [11] and under the assignment of $D_{s1}(2710)$ to the 2^3S_1 charmed-strange meson, the $\Gamma(D_{s1}(2710) \to D^*K)/\Gamma(D_{s1}(2710) \to DK) = 0.91$ was obtained, which is close to the experimental value [48]. We also notice the recent work of $D_{sJ}(2860)$ [49], where they also proposed that $D_{s1}(2710)$ is the 2^3S_1 $c\bar{s}$ meson.

[1] We need to explain the reason why the 2^3S_1 charmed-strange meson is not completely excluded in Ref. [5]. In Ref. [5], the total decay width of $D_{s1}(2710)$ as the 2^3S_1 charmed-strange meson was calculated, which is 32 MeV. This value is obtained with the typical $R = 3.2$ GeV^{-1} value. As shown in Fig. 4 (d) in [5], the total decay width is strongly dependent on the R value due to node effects. If taking other typical R values which are not far away from 3.2 GeV^{-1}, the total decay width can reach up to the lower limit of the experimental width of $D_{s1}(2710)$.

Besides the above exploration in the framework of a conventional charmed-strange meson, the exotic state explanation to $D_{s1}(2710)$ was given in Ref. [15].

In the following, we include the mixing between 2^3S_1 and 1^3D_1 states to further discuss the mixing angle dependence of the decay behavior of $D_{s1}(2860)$. Here, $D_{s1}(2S)$ and $D_{s1}(2860)$ are the mixtures of 2^3S_1 and 1^3D_1 states, which satisfy the relation

$$\begin{pmatrix} |D_{s1}(2S)\rangle \\ |D_{s1}(2860)\rangle \end{pmatrix} = \begin{pmatrix} \cos\theta & \sin\theta \\ -\sin\theta & \cos\theta \end{pmatrix} \begin{pmatrix} |2^3S_1\rangle \\ |1^3D_1\rangle \end{pmatrix}. \quad (13)$$

The $2S$–$1D$ mixing angle should be small due to the relative large mass gap between the $2S$ and $1D$ states, where we take some typical values $\theta = 0°$, $\theta = 15°$, and $\theta = 30°$ to present our results. $\theta = 0°$ denotes that there is no $2S$–$1D$ mixing. In Fig. 2, we present the total and partial decay widths, which depend on the R value, where we show the results with three different typical θ values. In the left-top panel of Fig. 2, we list the total decay width of $D_{s1}(2860)$ and the comparison with the experimental data. When taking $2.4 < R < 3.6$ GeV^{-1}, the calculated total decay width varies from 130 to 235 MeV, which indicates the theoretically estimated total decay width of $D_{s1}(2860)$ can overlap with the experimental measurement. In addition, we also notice that the partial decay widths for the $D_s\eta$ and $D_s^*\eta$ channels are less than 10 MeV, while for the DK, D^*K, and DK^* decay modes, the corresponding partial decay widths vary from several 20 MeV to more than 100 MeV, which strongly depends on the value of a mixing angle.

In Ref. [12], the authors adopted a different convention for the $2S$–$1D$ mixing, where their $2S$–$1D$ mixing angle has a sign opposite to our scenario. Taking the same R value and mixing angle for $D_{s1}(2860)$, we obtain the partial decay widths of DK and D^*K are less than 10 MeV, while the calculated partial decay width of DK^* is more than 20 MeV, which is consistent with the results in Ref. [12].

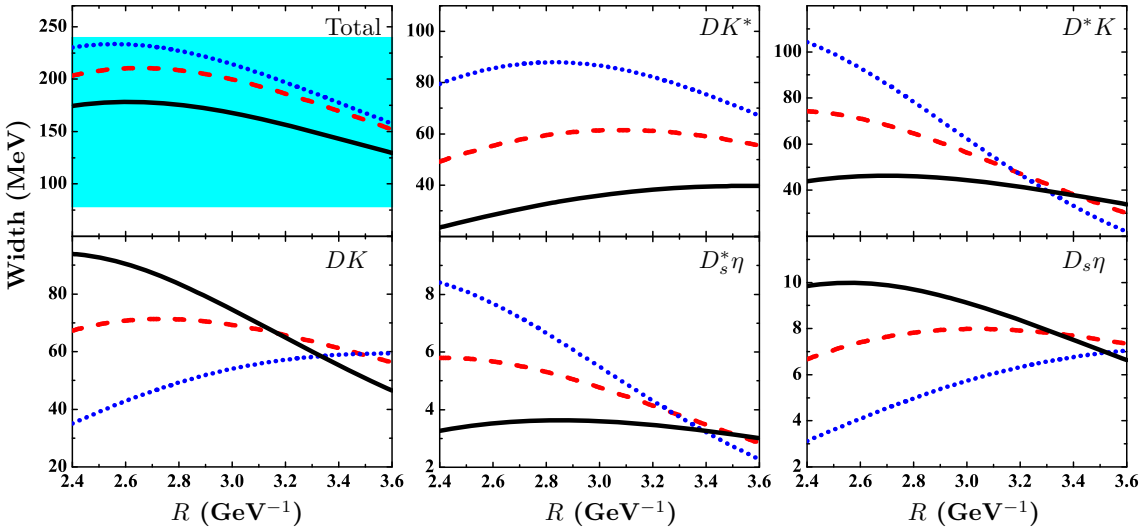

Fig. 2 The total and partial decay widths (in units of MeV) of $D_{s1}(2860)$ dependent on the R value. The *solid*, *dashed* and *dotted curves* correspond to the typical $2S$–$1D$ mixing angles $\theta = 0°, \theta = 15°$, and $\theta = 30°$, respectively. The *band in the left-top panel* is the total decay width with errors, which was reported by the LHCb Collaboration [1,2]

2.2 $D_{s3}(2860)$

The two-body OZI-allowed decay behavior of $D_{s3}(2860)$ as the 1^3D_3 charmed-strange meson is presented in the right panel of Fig. 1, where the obtained total width can reach up to 42 $\sim$ 60 MeV, which overlaps with the LHCb's data ($53 \pm 7 \pm 4 \pm 6$ MeV [1,2]). This fact further reflects that $D_{s3}(2860)$ is suitable for the 1^3D_3 charmed-strange meson. Similar to $D_{s1}(2860)$, the DK channel is also the dominant decay mode of $D_{s3}(2860)$, where the partial decay width of $D_{s3}(2860) \to DK$ is 25 $\sim$ 30 MeV in the selected R value range. Additionally, we also calculate the partial decay width of $D_{s3}(2860) \to D^*K$ and $D_{s3}(2860) \to DK^*$, which are 14 $\sim$ 24 and 0.9 $\sim$ 2.5 MeV, respectively. The partial decay widths for $D_s\eta$ and $D_s^*\eta$ channel are of order of 0.1 MeV. The corresponding typical ratios for $D_{s3}(2860)$ are

$$\frac{\Gamma(D_{s3}(2860) \to D^*K)}{\Gamma(D_{s3}(2860) \to DK)} = 0.55 \sim 0.80, \tag{14}$$

$$\frac{\Gamma(D_{s3}(2860) \to DK^*)}{\Gamma(D_{s3}(2860) \to DK)} = 0.03 \sim 0.09, \tag{15}$$

$$\frac{\Gamma(D_{s3}(2860) \to D_s\eta)}{\Gamma(D_{s1}(2860) \to DK)} = 0.018 \sim 0.020, \tag{16}$$

which can be tested in future experiment.

In Ref. [5], the ratio $\Gamma(D^*K)/\Gamma(DK) = 13/22 = 0.59$ was given for $D_{sJ}(2860)$ observed by Belle as the 1^3D_3 state, where the QPC model was also adopted and this ratio is obtained by taking a typical value $R = 2.94$ GeV^{-1}. In the present work, we consider the range $R = 2.4 \sim 3.6$ GeV^{-1} to present the D^*K/DK ratio for $D_{s3}(2860)$. If comparing the ratio given in Eq. (14) with the corresponding one obtained in Ref. [5], we notice that their value $\Gamma(D^*K)/\Gamma(DK) = 0.59$ [5] just falls into our obtained range $\Gamma(D^*K)/\Gamma(DK) = 0.55 \sim 0.80$.

In addition, we need to make a comment on the experimental ratio $\Gamma(D^*K)/\Gamma(DK) = 1.10 \pm 0.15 \pm 0.19$ for $D_{sJ}(2860)$, which was extracted by the BaBar Collaboration [3]. Since LHCb indicated that there exist two resonances $D_{s1}(2860)$ and $D_{s3}(2860)$ in the DK invariant mass spectrum [1,2], the experimental ratio $\Gamma(D^*K)/\Gamma(DK)$ for $D_{sJ}(2860)$ must be changed, which means that we cannot simply apply the old $\Gamma(D^*K)/\Gamma(DK)$ data in Ref. [3] to draw a conclusion on the structure of $D_{sJ}(2860)$. We expect further experimental measurements of this ratio, which will be helpful to reveal the properties of the observed $D_{sJ}(2860)$ states.

2.3 $1D(2^-)$ and $1D'(2^-)$

In the following, we discuss the decay behaviors of the two missing $1D$ states in the present experiment, which is crucial to the experimental search for the $1D(2^-)$ and $1D'(2^-)$ states.

We first fix the mixing angle $\theta_{1D} = 39°$ obtained in the heavy quark limit, and discuss the R value dependence of the total and partial decay widths of the two missing 2^- states in experiment, which are presented in Fig. 3. Since these two $1D$ states have not yet been seen in experiment, we take the mass range 2850 $\sim$ 2950 MeV, which covers the theoretically predicted masses of the $1D(2^-)$ and $1D'(2^-)$ states from different groups listed in Table 1, to discuss the decay behaviors of the $1D(2^-)$ and $1D'(2^-)$ states.

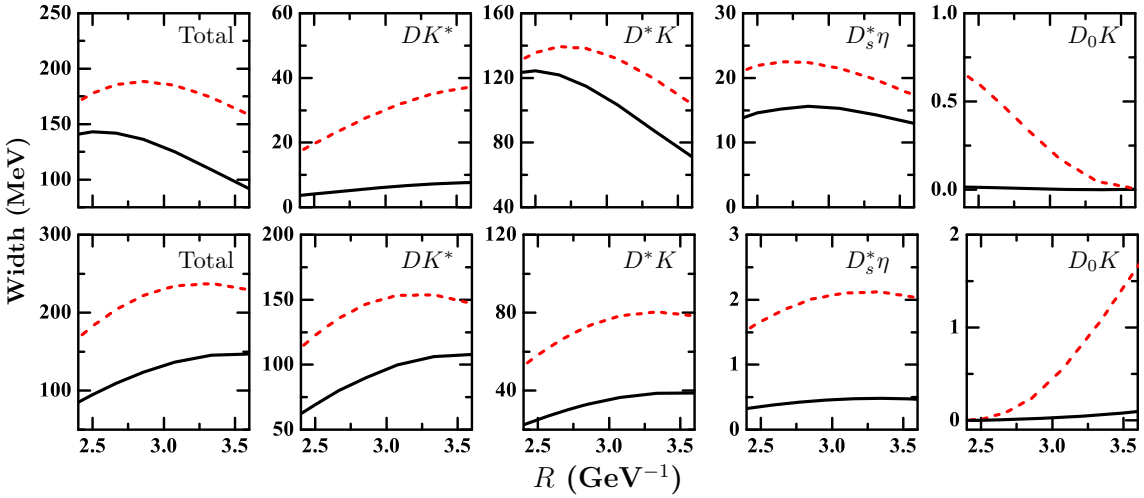

Fig. 3 The total and partial decay widths of the $1D(2^-)$ (*upper row*) and the $1D'(2^-)$ (*lower row*) charmed-strange mesons dependent on the R values. Here, a mixing angle of 39° is chosen. The *solid* and *dashed curves* correspond to two predicted masses of 2^- states, 2850 and 2950 MeV, respectively

The total and partial decay widths of $1D(2^-)$ are present in the upper panel of Fig. 3. Here, two typical masses of the $1D(2^-)$ state, 2850 and 2950 MeV, are considered, which are corresponding to the solid and dashed curved in Fig. 3. The estimated total decay width varies from 90 to 190 MeV, which is due to the uncertainty of the predicted mass of the $1D(2^-)$ state and the R value dependence as mentioned above. If the mass of the $1D(2^-)$ state can be constrained by future experiment, the uncertainty of the total width for the $1D(2^-)$ state can be further reduced. In any case, our study indicates that the $1D(2^-)$ state has a broad width.

Additionally, as shown in Fig. 3, the $1D(2^-)$ state can dominantly decay into D^*K, where $\mathcal{B}(1D(2^-) \to D^*K) = (77 \sim 87)\,\%$, and DK^* and $D_s^*\eta$ are its main decay modes. Comparing D^*K, DK^*, and $D_s^*\eta$ with each other, $D_s^*\eta$ is the weakest decay channel. Hence, we suggest experimental search for the $1D(2^-)$ state firstly via the D^*K channel.

We also obtain two typical ratios, i.e.,

$$\frac{\Gamma(1D(2^-) \to DK^*)}{\Gamma(1D(2^-) \to D^*K)} = 0.11 \sim 0.36, \tag{17}$$

$$\frac{\Gamma(1D(2^-) \to D_s^*\eta)}{\Gamma(1D(2^-) \to D^*K)} = 0.11 \sim 0.18, \tag{18}$$

which can be accessible in experiment.

As for the $1D'(2^-)$ state, the total and partial decay width are present in the lower panel of Fig. 3. We predict its total decay width ((80 ∼ 240) MeV), which shows that the $1D'(2^-)$ state is also a broad resonance, where DK^* is its dominant decay mode with a branching ratio $\mathcal{B}(1D'(2^-) \to DK^*) = (64 \sim 73)\,\%$. Its main decay mode includes D^*K, while $1D' \to D_s^*\eta$ and $1D' \to D_0(2400)K$ have small partial decay widths. Besides the above information, two typical ratios are listed:

$$\frac{\Gamma(1D'(2^-) \to D^*K)}{\Gamma(1D'(2^-) \to DK^*)} = 0.36 \sim 0.53, \tag{19}$$

$$\frac{\Gamma(1D'(2^-) \to D^*\eta)}{\Gamma(1D'(2^-) \to DK^*)} = 0.004 \sim 0.013. \tag{20}$$

It should be noticed that the threshold of $D_{s0}^*(2317)\eta$ is 2865 MeV and two $1D$ charmed-strange mesons with $J^P = 2^-$ decaying into $D_{s0}^*(2317)\eta$ occur via a $D-$ wave. Thus, $1D(2^-)/1D'(2^-) \to D_{s0}^*(2317)\eta$ is suppressed, which is supported by our calculation since the corresponding partial decay widths are of the order of a few keV for $1D(2^-) \to D_{s0}^*\eta$ and of the order of 0.1 keV for $1D'(2^-) \to D_{s0}^*\eta$.

In Table 4, we fix the R value of $1D(2^-)$ and $1D'(2^-)$ to be 2.85 GeV^{-1} [46] and further discuss the total and partial decay widths dependent on the mixing angle θ_{1D}, where three typical values $\theta_{1D} = 20°$, $\theta_{1D} = 30°$, and $\theta_{1D} = 50°$ are adopted. For the $1D(2^-)$ state, its total decay width varies from 152 to 187 MeV, which indicates that the total decay width is weakly dependent on the mixing angle θ_{1D}. Moreover, the $1D(2^-)$ state dominantly decays into D^*K, whose width varies from 110 to 134 MeV caused by the uncertainty of the mass of the $1D(2^-)$ state and the different mixing angle θ_{1D}. In addition, the ratio of $1D(2^-) \to D_s^*\eta$ and $1D(2^-) \to D^*K$ is estimated to be $0.11 \sim 0.19$, which is consistent with that shown in Eq. (18). However, the predicted partial decay width of $1D(2^-) \to DK^*$ is strongly dependent on the mixing angle, which varies from 2 to 56 MeV.

The total decay width of $1D'(2^-)$ varies from 117 to 230 MeV depending on different predicted masses and mixing angles. Its dominant decay modes are D^*K and DK^*, and the ratios of $1D'(2^-) \to D^*K$ and $1D'(2^-) \to DK^*$ are predicted to be $0.39 \sim 0.66$. The partial decay widths of $1D'(2^-) \to D_s^*\eta$ and $1D'(2^-) \to D_0(2400)K$ are rel-

Table 4 The total and partial decay widths of two 2^- states (in units of MeV) dependent on the mixing angle θ_{1D} (the typical values are $\theta_{1D} = 20°$, $30°$, and $50°$). Here, the R value of $1D(2^-)$ and $1D'(2^-)$ is fixed as $R = 2.85\ \text{GeV}^{-1}$ [46]

	M=2850 MeV						M=2950 MeV					
	$\theta_{1D} = 20°$		$\theta_{1D} = 30°$		$\theta_{1D} = 50°$		$\theta_{1D} = 20°$		$\theta_{1D} = 30°$		$\theta_{1D} = 50°$	
Channels	$1D(2^-)$	$1D'(2^-)$	$1D(2^-)$	$1D'(2^-)$	$1D(2^-)$	$1D'(2^-)$	$1D(2^-)$	$1D'(2^-)$	$1D(2^-)$	$1D'(2^-)$	$1D(2^-)$	$1D'(2^-)$
D^*K	126.93	44.60	135.61	35.90	134.62	36.84	110.42	77.82	113.85	74.39	113.46	74.76
DK^*	26.06	70.04	13.54	82.59	1.99	94.18	56.19	118.06	38.58	135.69	22.34	152.00
$D_s^*\eta$	13.93	2.08	15.17	0.83	15.03	0.97	20.23	4.21	21.91	2.54	21.72	2.72
$D_0^*(2400)\,K$	0.012	0.011	0.008	0.015	0.002	0.022	0.50	0.08	0.42	0.16	0.22	0.36
Total	166.93	116.73	164.33	119.34	151.64	132.01	187.34	200.17	174.76	212.78	157.74	229.84

atively small and are given by several MeV and less than 0.5 MeV, respectively.

3 Discussion and conclusions

With the observation of two charmed-strange resonances $D_{s1}(2860)$ and $D_{s3}(2860)$, which was recently announced by the LHCb Collaboration [1,2], the observed charmed-strange states become more and more abundant. In this work, we have carried out a study of the observed $D_{s1}(2860)$ and $D_{s3}(2860)$, which indicates that $D_{s1}(2860)$ and $D_{s3}(2860)$ can be well categorized as 1^3D_1 and 1^3D_3 states in the charmed-strange meson family since the experimental widths of $D_{s1}(2860)$ and $D_{s3}(2860)$ can be reproduced by the corresponding calculated total widths of the 1^3D_1 and 1^3D_3 states. In addition, the result of their partial decay widths shows that the DK decay mode is dominant both for 1^3D_1 and 1^3D_3 states, which naturally explains why $D_{s1}(2860)$ and $D_{s3}(2860)$ were first observed in the DK channel. If $D_{s1}(2860)$ and $D_{s3}(2860)$ are the 1^3D_1 and 1^3D_3 states, respectively, our study also indicates that the D^*K and DK^* channels are the main decay mode of $D_{s1}(2860)$ and $D_{s3}(2860)$, respectively. Thus, we suggest for future experiments to search for $D_{s1}(2860)$ and $D_{s3}(2860)$ in these main decay channels, which cannot only test our prediction presented in this work but also provide more information of the properties of $D_{s1}(2860)$ and $D_{s3}(2860)$.

As the spin partners of $D_{s1}(2860)$ and $D_{s3}(2860)$, two $1D$ charmed-strange mesons with $J^P = 2^-$ are still missing in experiment. Thus, in this work we also predict the decay behaviors of these two missing $1D$ charmed-strange mesons. Our calculation by the QPC model shows that both the $1D(2^-)$ and the $1D'(2^-)$ states have very broad widths. For the $1D(2^-)$ and $1D'(2^-)$ states, their dominant decay mode is D^*K and DK^*, respectively. In addition, DK^* and D^*K are also the important decay modes of the $1D(2^-)$ and $1D'(2^-)$ states, respectively. This investigation provides valuable information when further experimentally exploring these two missing $1D$ charmed-strange mesons.

In summary, the observed $D_{s1}(2860)$ and $D_{s3}(2860)$ provide us a good opportunity to establish higher states in the charmed-strange meson family. The following experimental and theoretical efforts are still necessary to reveal the underlying properties of $D_{s1}(2860)$ and $D_{s3}(2860)$. Furthermore, it is a challenging research topic for future experiments to hunt the two predicted missing $1D$ charmed-strange mesons with $J^P = 2^-$.

Before closing this section, we would like to discuss the threshold effect or coupled-channel effect, which was proposed to solve the puzzling lower mass and narrow widths for $D_{s0}(2317)$ [50] and $D_{s1}(2460)$ [51], and to understand the properties of $X(3872)$. We notice that there exist several typical D^*K, DK^*, and D^*K^* thresholds, which are ∼2580, ∼2762, and ∼2902 MeV, respectively. Here, the observed $D_{s1}(2860)$ and $D_{s3}(2860)$ are near the D^*K^* threshold while $D_{s1}(2715)$ is close to the DK^* threshold. This fact also shows that the threshold effect or coupled-channel effect is important to these observed charmed-strange states. For example, in Ref. [52], the authors studied the D^*K^* threshold effect on $D_{s2}^*(2573)$. Thus, further theoretical study of $D_{s1}(2860)$ and $D_{s3}(2860)$ by considering the threshold effect or coupled-channel effect is an interesting research topic.

In addition, the results presented in this work are calculated by using the SHO wave functions with a rms radius obtained within a relativistic quark model [18], which can provide a quantitative estimate of the decay behavior of hadrons. However, the line shape of the SHO wave function is slightly different from the one obtained by the relativistic quark model. For example, the nodes may appear at different places for these two cases. Thus, adopting a numerical wave function from a relativistic quark model [18] may further improve the whole results, where we can compare the results obtained by using the SHO wave function and the numerical wave function, which is an interesting research topic.[2]

[2] We would like to thank the anonymous referee for his/her valuable suggestion.

Acknowledgments This project is supported by the National Natural Science Foundation of China under Grants No. 11222547, No. 11375240, No. 11175073, and No. 11035006, the Ministry of Education of China (SRFDP under Grant No. 2012021111000), and the Fok Ying Tung Education Foundation (No. 131006).

References

1. R. Aaij et al., LHCb Collaboration, arXiv:1407.7574 [hep-ex]
2. R. Aaij et al., LHCb Collaboration, arXiv:1407.7712 [hep-ex]
3. B. Aubert et al., BaBar Collaboration, Phys. Rev. Lett. **97**, 222001 (2006). hep-ex/0607082
4. B. Aubert et al., BaBar Collaboration, Phys. Rev. D **80**, 092003 (2009). arXiv:0908.0806 [hep-ex]
5. B. Zhang, X. Liu, W.-Z. Deng, S.-L. Zhu, Eur. Phys. J. C **50**, 617 (2007). hep-ph/0609013
6. P. Colangelo, F. De Fazio, S. Nicotri, Phys. Lett. B **642**, 48 (2006). hep-ph/0607245
7. P. Colangelo, F. De Fazio, F. Giannuzzi, S. Nicotri, Phys. Rev. D **86**, 054024 (2012). arXiv:1207.6940 [hep-ph]
8. D. -M. Li, B. Ma, Y.-H. Liu, Eur. Phys. J. C **51**, 359 (2007). hep-ph/0703278
9. X.-H. Zhong, Q. Zhao, Phys. Rev. D **81**, 014031 (2010). arXiv:0911.1856 [hep-ph]
10. B. Chen, D.-X. Wang, A. Zhang, Phys. Rev. D **80**, 071502 (2009). arXiv:0908.3261 [hep-ph]
11. P. Colangelo, F. De Fazio, S. Nicotri, M. Rizzi, Phys. Rev. D **77**, 014012 (2008). arXiv:0710.3068 [hep-ph]
12. D.-M. Li, B. Ma, Phys. Rev. D **81**, 014021 (2010). arXiv:0911.2906 [hep-ph]
13. X.-H. Zhong, Q. Zhao, Phys. Rev. D **78**, 014029 (2008). arXiv:0803.2102 [hep-ph]
14. E. van Beveren, G. Rupp, Phys. Rev. D **81**, 118101 (2010). arXiv:0908.1142 [hep-ph]
15. J. Vijande, A. Valcarce, F. Fernandez, Phys. Rev. D **79**, 037501 (2009). arXiv:0810.4988 [hep-ph]
16. Z.-F. Sun, X. Liu, Phys. Rev. D **80**, 074037 (2009). arXiv:0909.1658 [hep-ph]
17. J. Beringer et al., Particle Data Group Collaboration, Phys. Rev. D **86**, 010001 (2012)
18. S. Godfrey, N. Isgur, Phys. Rev. D **32**, 189 (1985)
19. T. Matsuki, T. Morii, K. Sudoh, Prog. Theor. Phys. **117**, 1077 (2007). hep-ph/0605019
20. M. Di Pierro, E. Eichten, Phys. Rev. D **64**, 114004 (2001). hep-ph/0104208
21. D. Ebert, R.N. Faustov, V.O. Galkin, Eur. Phys. J. C **66**, 197 (2010). arXiv:0910.5612 [hep-ph]
22. T. Matsuki, T. Morii, K. Seo, Prog. Theor. Phys. **124**, 285 (2010). arXiv:1001.4248 [hep-ph]
23. L. Micu, Nucl. Phys. B **10**, 521 (1969)
24. A. Le Yaouanc, L. Oliver, O. Pene, J.C. Raynal, Phys. Rev. D **8**, 2223 (1973)
25. A. Le Yaouanc, L. Oliver, O. Pene, J.C. Raynal, Phys. Rev. D **9**, 1415 (1974)
26. A. Le Yaouanc, L. Oliver, O. Pene, J.C. Raynal, Phys. Rev. D **11**, 1272 (1975)
27. A. Le Yaouanc, L. Oliver, O. Pene, J.C. Raynal, Phys. Lett. B **72**, 57 (1977)
28. A. Le Yaouanc, L. Oliver, O. Pene, J.C. Raynal, Phys. Lett. B **71**, 397 (1977)
29. A. Le Yaouanc, L. Oliver, O. Pene, J.C. Raynal, (Gordon and Breach, New York, 1988), p. 311
30. E. van Beveren, C. Dullemond, G. Rupp, Phys. Rev. D **21**, 772 (1980) (erratum-ibid. D 22, 787, 1980)
31. E. van Beveren, G. Rupp, T.A. Rijken, C. Dullemond, Phys. Rev. D **27**, 1527 (1983)
32. R. Bonnaz, B. Silvestre-Brac, C. Gignoux, Eur. Phys. J. A **13**, 363 (2002). hep-ph/0101112
33. W. Roberts, B. Silvestre-Brac, Few Body Syst. **11**, 171 (1992)
34. X. Liu, Z.-G. Luo, Z.-F. Sun, Phys. Rev. Lett. **104**, 122001 (2010). arXiv:0911.3694 [hep-ph]
35. Z.-F. Sun, J.-S. Yu, X. Liu, T. Matsuki, Phys. Rev. D **82**, 111501 (2010). arXiv:1008.3120 [hep-ph]
36. J.-S. Yu, Z.-F. Sun, X. Liu, Q. Zhao, Phys. Rev. D **83**, 114007 (2011). arXiv:1104.3064 [hep-ph]
37. X. Wang, Z.-F. Sun, D.-Y. Chen, X. Liu, T. Matsuki, Phys. Rev. D **85**, 074024 (2012). arXiv:1202.4139 [hep-ph]
38. Z.-C. Ye, X. Wang, X. Liu, Q. Zhao, Phys. Rev. D **86**, 054025 (2012). arXiv:1206.0097 [hep-ph]
39. L.-P. He, X. Wang, X. Liu, Phys. Rev. D **88**, 034008 (2013). arXiv:1306.5562 [hep-ph]
40. Y. Sun, X. Liu, T. Matsuki, Phys. Rev. D **88**(9), 094020 (2013). arXiv:1309.2203 [hep-ph]
41. Y. Sun, Q.-T. Song, D.-Y. Chen, X. Liu, S.-L. Zhu, Phys. Rev. D **89**, 054026 (2014). arXiv:1401.1595 [hep-ph]
42. C.-Q. Pang, L.-P. He, X. Liu, T. Matsuki, Phys. Rev. D **90**, 014001 (2014). arXiv:1405.3189 [hep-ph]
43. L.-P. He, D.-Y. Chen, X. Liu, T. Matsuki, arXiv:1405.3831 [hep-ph]
44. M. Jacob, G. C. Wick, Ann. Phys. **7**, 404 (1959). (Ann Phys, 281, 774, 2000)
45. S. Godfrey, R. Kokoski, Phys. Rev. D **43**, 1679 (1991)
46. F.E. Close, E.S. Swanson, Phys. Rev. D **72**, 094004 (2005). hep-ph/0505206
47. H.G. Blundell, arXiv:hep-ph/9608473
48. J. Brodzicka et al., Belle Collaboration, Phys. Rev. Lett. **100**, 092001 (2008.) arXiv:0707.3491 [hep-ex]
49. S. Godfrey, K. Moats, arXiv:1409.0874 [hep-ph]
50. E. van Beveren, G. Rupp, Phys. Rev. Lett. **91**, 012003 (2003). hep-ph/0305035
51. E. van Beveren, G. Rupp, Eur. Phys. J. C **32**, 493 (2004). hep-ph/0306051
52. R. Molina, T. Branz, E. Oset, Phys. Rev. D **82**, 014010 (2010). arXiv:1005.0335 [hep-ph]